UMYU Scientifica, Vol. 4 NO. 2, June 2025, Pp 298 – 308
https://doi.org/10.56919/usci.2542.029
ISSN: 2955 – 1145 (print); 2955 – 1153 (online)
A periodical of the Faculty of Natural and Applied Sciences, UMYU, Katsina

ORIGINAL RESEARCH ARTICLE

Chromatographic and Spectroscopic Characterization and Identification of Compounds in Flavonoid-Rich Fraction of *Thesium viride* A.W.Hill

Sani Shehu[1]*, Uwaisu Iliyasu[1], Peter Waziri[2], Abubakar Abdulrazak[3] and Kola' Kayode Ajibesin[4]

[1]Department of Pharmacognosy and Drug Development, Kaduna State University, Kaduna, Nigeria
[2]Department of Biochemistry and Biotechnology, Kaduna State University, Kaduna, Nigeria
[3]Department of Human Physiology, Kaduna State University, Kaduna, Nigeria
[4]Department of Pharmacognosy and Herbal Medicine, Niger Delta University, Wilberforce Island, Bayelsa, Nigeria

ABSTRACT

Thesium viride A.W.Hill is a hemi-parasite subshrub from the Santalaceae family. The aerial part of the plant is utilised in the treatment of jaundice, liver enlargement, splenomegaly, and ulcers. It is been reported that the ethyl acetate (flavonoid-rich) fraction has stronger antibacterial and antioxidant properties than the 70% ethanol extract and other fractions. This research aims to develop a chromatographic fingerprint and isolate bioactive compounds from the flavonoid-rich fraction of *T. viride* that may be responsible for its activity. The plant's aerial portion was collected, allowed to air dry in the shade, and then reduced in size into powder. It was macerated with 70% ethanol, and subsequently portioned using n-hexane, ethyl acetate, and n-butanol, leaving an aqueous residue. Fourier-transform infrared (FTIR), ultraviolet (UV) spectroscopy, and column chromatography were performed on the flavonoid-rich fraction, resulting in the isolation of two constituents, which were subjected to nuclear magnetic resonance (NMR) experiments for complete elucidation of their chemical structures. The UV and FTIR fingerprint profile of the flavonoid-rich fraction has been developed and can be used for identification and quality control of the fraction of *T. viride*. Two chemical compounds were first reported to be isolated from the flavonoid-rich fraction and characterized as 1-heptacosanol and Quercetin. The chromatographic and spectroscopic fingerprint serves as a quality control for the standardization of the flavonoid-rich fraction of *T. viride*. These compounds isolated may be responsible for the antimicrobial, antiulcer, antioxidant, and hepatoprotective activities of *T. viride*.

ARTICLE HISTORY

Received April 27, 2025
Accepted June 28, 2025
Published June 30, 2025

KEYWORDS

Thesium viride, Flavonoids, Flavonol, 1-heptacosanol, Quercetin

INTRODUCTION

Phytochemicals are naturally occurring biologically active compounds present in whole plants, fruits, seeds, and other morphological parts. They serve as protective to the plant from pollution, dehydration, and ultraviolet radiation (Guemari et al., 2022). Analysing these chemical constituents of plants to determine their potential medicinal uses is known as phytochemical screening (Kaur et al., 2022).

Thesium viride A.W.Hill is a hemiparasite subshrub also known as "Huntu' by Hausas of northern Nigeria and belongs to the family Santalaceae (Shehu & Iliyasu, 2017; Shehu et al., 2016a). It is widely distributed in Africa, Madagascar, and South America (Zhigila et al., 2020). The plant is used for to treat jaundice, liver enlargement, splenomegaly, and ulcers (Iwu, 2014; Shehu et al., 2017; Shehu et al., 2017).

Preliminary screening of aqueous ethanol extract showed the presence of phenolics, flavonoids, alkaloids, and glycosides (Shehu et al., 2017; Shehu et al., 2016a). Recently, some bioactive compounds, such as bis-(2-ethylhexyl) phthalate, octadecenoic acid isomers, and diethyl phthalate, were detected in the extract of *T. viride* (Mustapha et al., 2023).

Solvent-solvent portioning of 70% aqueous ethanol extract with hexane, ethyl acetate, and n-butanol by Shehu et al (2022a) reported that the highest amount of flavonoid content was found in ethyl acetate fraction (103.29 mg.QE/g) followed by the 70% aqueous ethanol extract, butanol, and aqueous fraction at 87.62, 79.79 and 18.17 mg.QE/g respectively.

The ethyl acetate fraction of *T. viride* demonstrated antimicrobial activity against *S. faecalis, S. aureus, S.*

Correspondence: Sani Shehu. Department of Pharmacognosy and Drug Development, Kaduna State University, Kaduna, Nigeria. ✉ pharmsani@gmail.com.

How to cite: Shehu, S., Iliyasu, U., Waziri, P., Abdulrazak, A., & Ajibesin, K. K. (2025). Chromatographic and Spectroscopic Characterization and Identification of Compounds in Flavonoid-Rich Fraction of *Thesium viride* A.W.Hill. *UMYU Scientifica*, 4(2), 298 – 308. https://doi.org/10.56919/usci.2542.029

dysenteriae, E. coli, H. pylori, and *Candida krusei* (Shehu et al., 2016a; Shehu et al., 2016b).

The ethyl acetate fraction was found to have the highest antioxidant capacity in DPPH, FRAP, and TAC, which was attributed to the presence of phenolics and flavonoids (Shehu et al., 2022a). Shehu et al. (2022b) reported the liver protective activity of extracts and fractions of *T. viride* in CCl_4-induced liver damage, in which the fractions showed a higher reduction of elevated cytosolic AST and alanine ALT toward normal in a dose-dependent manner.

Despite the potential bioactivity of the ethyl acetate fraction of *T. viride*, there is a gap in the phytochemical profiling and isolation of chemical constituents from the fraction. The aim of this research was to develop a spectroscopic fingerprint, isolate bioactive compounds from the flavonoid-rich (ethyl acetate) fraction, and elucidate the chemical structure of the isolated compounds of *T. viride.* These was the first time the flavonoid-rich fraction of *T. viride* was chemically profile with isolation and elucidation of 1-heptacosanol and Quercetin.

MATERIAL AND METHODS

Plant collection, extraction, and fractionation:

The plant was obtained at Kawo market, Kaduna, and was identified and authenticated with voucher number of KASU/PCG/HERB/300 at the Herbarium Unit of the Department of Pharmacognosy and Drug Development, Kaduna State University, Kaduna. Powdered dried aerial part of plant (1 kg) was extracted by maceration with of 70%v/v ethanol in a glass jar for 72 hours. Extract was filtered, concentrated in a rotary evaporator at 30 °C, and evaporated to dryness on a water bath at 60 °C.

Fractionation of aqueous ethanol extract: The aqueous ethanol extract (130 g) was dissolved in distilled water (300 mL) and successively partitioned in a separating funnel exhaustively with n-hexane, ethyl acetate, and n-butanol (Madeleine et al., 2019). The flavonoid-rich (ethyl acetate) fraction was concentrated in vacuo at 30 °C .

Column chromatography of flavonoid-rich fraction of *T. viride:* The fraction (1 g) was pre-adsorbed with about 2 g of silica gel, which was then allowed to dry. It was then loaded on the column and eluted with 200 mL of 100% n-hexane at 2 mL/min. 20 mL in each aliquot was collected. Thereafter, the polarity of eluting solvent was increased to 95%, 90%, and 85% (hexane/ethyl acetate) for many collections. Based on the TLC profile, the solvent system polarity was either maintained or increased using ethyl acetate. The various column fractions having similar TLC profiles were pooled together and labelled A to K. Bulked fractions B&C were subjected to preparative TLC.

Preparative TLC of B&C bulked fractions: The mobile phase (100 mL) hexane/ethyl acetate (2:3) was prepared and introduced into the chromatographic tank, which was allowed to saturate for 30 min. B&C was streaked horizontally on a glass Prep TLC (Silica Gel 60 F254 20x20 cm size 1 mm thick) as a band and allowed to dry. The plate was then introduced into the tank and developed. The single band identified on daylight was then scraped, eluted in ethyl acetate (100%), centrifuged, filtered, concentrated, and finally obtained and labelled as KHA.

UV and FTIR Spectroscopic analysis of flavonoid-rich fraction and column fraction B&C

Ultraviolet-visible (UV-VIS): The fractions were diluted to 1:10 with methanol and scanned using a double-beam UV-spectrophotometer (PerkinElmer, USA) to detect the characteristic peaks at wavelengths of 200 to 800 nm. The peak values of the UV were recorded (Jain et al., 2016).

Fourier-transform infrared (FTIR): Ten (10) mg of the dried fractions were encapsulated in 100 mg of KBr pellet for a translucent sample discs. The powdered sample of each fraction was loaded and scanned 4000-650 cm^{-1} by 25 scans and a resolution of 4 cm^{-1} in a FTIR spectroscope and peak values recorded (Donkor *et al.*, 2019).

NMR Spectroscopy of isolated compounds: The NMR spectroscopy was carried out on isolated compounds HAJ and KHA. The analysis involve 1D (1H, and 13C) and 2D (HSQC). The analysis was conducted on an Agilent 400MHz with residual solvent peaks as internal standard. The chemical shift values were expressed in parts per million (ppm). Deutrated chloroform and deutrated acetone were used as NMR solvents for HAJ and KHA, respectively (Zuchowski et al., 2014). The NMR spectra obtained were used for the structure elucidation of compounds.

RESULTS

Column Chromatography of Flavonoid-rich Fraction

Table 1: Pooled Column Fractions developed in Hexane/Ethyl acetate (2:3)

Column Fractions	Code
1-2	-
3	HAJ
4-9	A
10-17	B
18-23	C
24-26	D
27-29	E
30-33	F
34-36	G
37-49	H
50-54	I
55-57	J
58-57	K

Column chromatography of the flavonoid-rich fraction resulted in the collection of 70 column fractions, which were monitored based on their TLC profile. Column fraction 3 was found to contain a single spot of compound labelled HAJ, a white powder soluble in chloroform and insoluble in acetone and methanol with a melting point of 81-83°C. The column fractions with similar

chromatograms were pooled together and labelled A-K as shown in Table 1.

Compound KHA was obtained from the preparative TLC of B&C bulked fractions. An amorphous yellow powder soluble in acetone and methanol, reacted positively with ferric chloride and aluminum chloride, and has a melting point of 309-311^{0}C. The UV-spectroscopy of the flavonoid-rich fraction and column fraction (B&C) of *T. viride* was done at a range of 200 to 800 nm. Flavonoid-rich fraction shows absorption maxima at 256, 368, 505, and 658nm. While the column fraction B&C shows a double peak at 255 and 371 nm, as shown in Table 2.

Spectroscopic fingerprint of flavonoid-rich fraction and Column Fraction B&C

FTIR spectra of flavonoid-rich fraction show a prominent peak at 3694 and 3240 cm^{-1}, absorption bands in the region 2922/2855 cm^{-1}, 1654/1603 cm^{-1}, and bending vibration at 1443 cm^{-1} and band at 787 cm^{-1} as shown in Figure 1. The FTIR spectra of column fraction (Figure 2) show a broad peak at 3220 cm^{-1}, a band observed at 1655/1606 cm^{-1}, and peaks at 1500/1400 cm^{-1} and 1163/1092 cm^{-1}.

Nuclear Magnetic Resonance Spectroscopy of Isolated Compounds

NMR spectra of compound HAJ

^{1}H NMR spectrum of compound HAJ

The ^{1}HNMR suggested a triplet signal at δ 3.66 (2H, J = 6.8), a multiplet signal at δ 1.61 (4H, m) and an intense peak at δ 1.24 showing up as a multiplet integrated for 46 protons and an upfield signal at δ 0.88 (3H, t, J = 6.8 Hz) which is diagnostic a terminal methyl group as shown in Figure 3.

^{13}C NMR spectrum of compound HAJ

The ^{13}C-NMR showed the presence of methylenes and one methyl signal. An observed signal at δ 62.4 (C-1) is an oxygenated methylene carbon. Signals due to methylene carbons in the aliphatic regions at δ 32.8, 31.9, 29.7, 29.6, 29.4, 29.3, 25.7, and 22.7 were also displayed. The intense signal at δ 29.7 is due to overlapping methylene carbons. The signal at δ 14.1 is attributed to the terminal methyl group, as shown in Figure 4.

Table 2: The Number of UV-VIS Absorption Peaks and Wavelength from Flavonoid-rich and Column Fraction B&C

Fractions	No. of absorption peaks	Wavelength (nm)
Flavonoid-rich fraction	4	256
		368
		505
		658
Column fraction B&C	2	255
		371

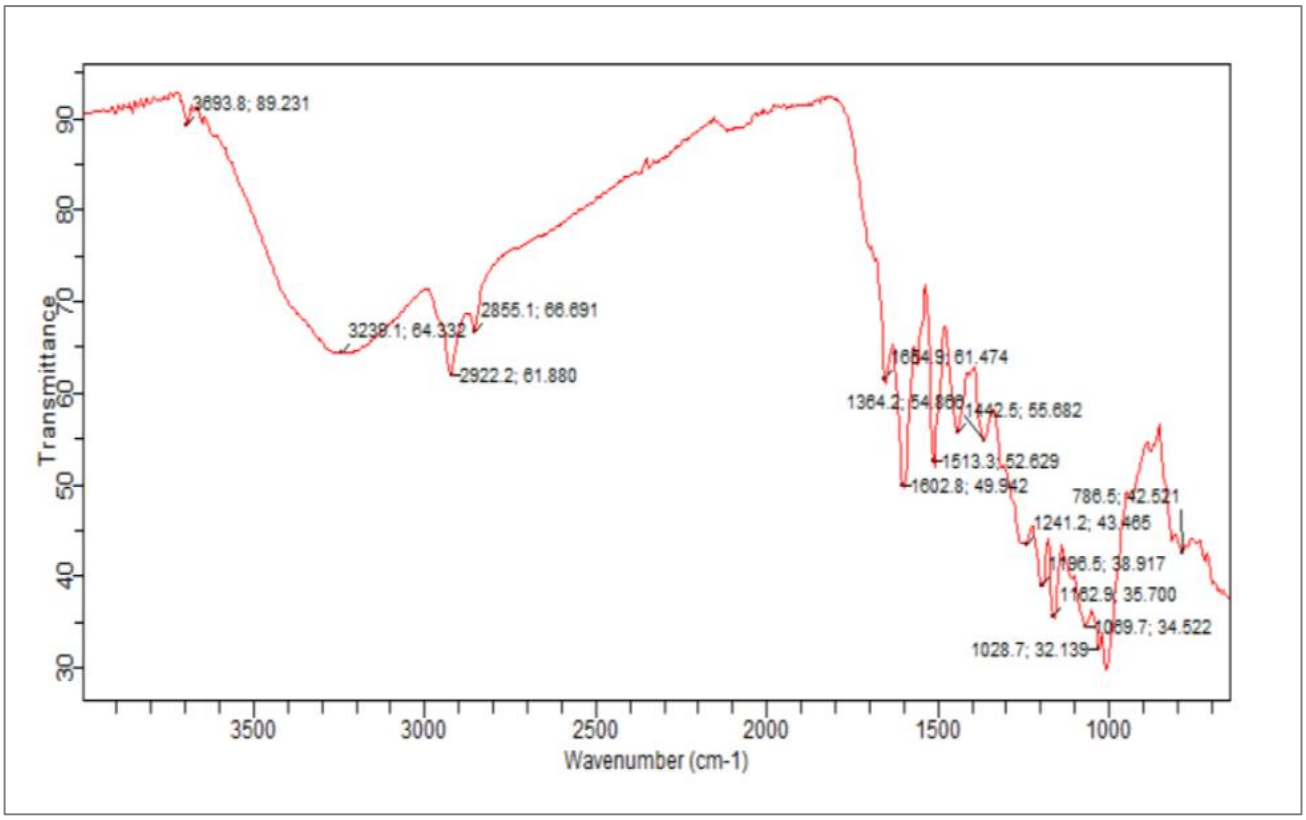

Figure 1: FTIR Spectra of Flavonoid-rich Fraction of *T. viride*.

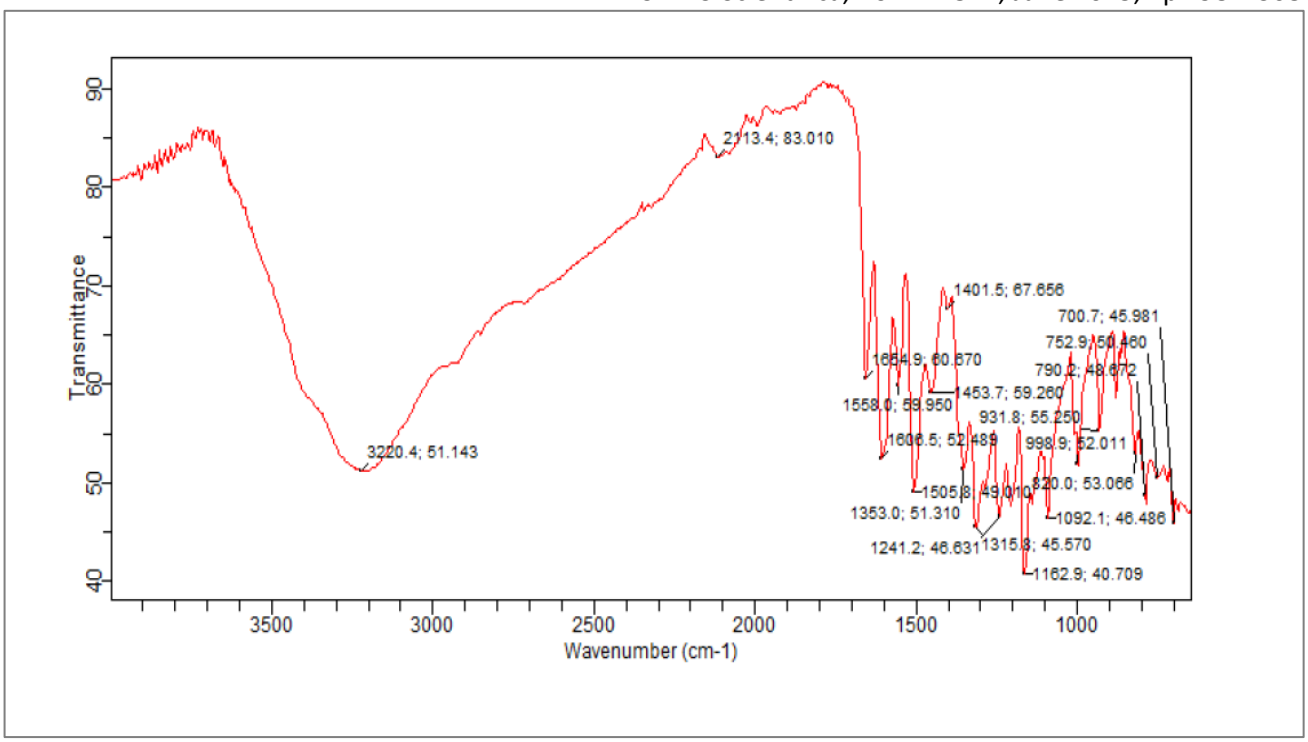

Figure 2: FTIR Spectra of Column Fraction B&C of *T. viride*

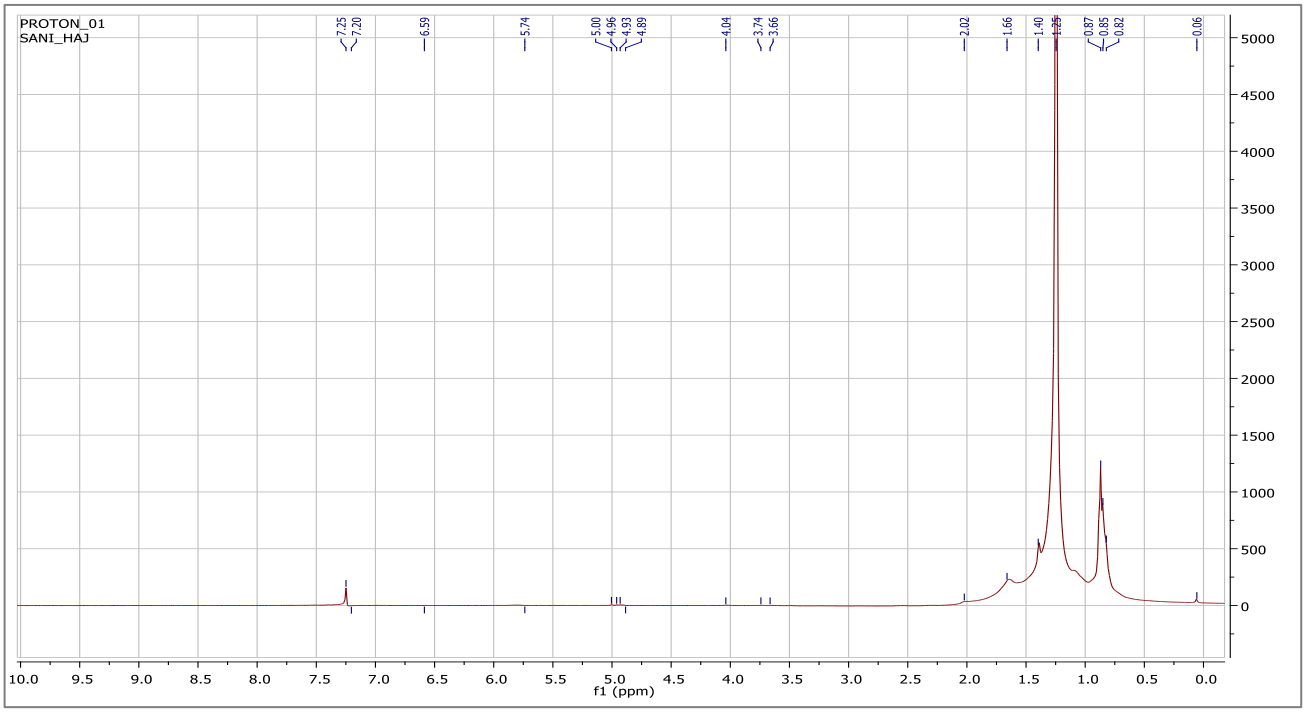

Figure 3: Proton NMR Spectra of HAJ Isolated from *T. viride* in Deteurated Chloroform

Table 3: Comparison between Chemical Shift Data of HAJ from *T. viride* and that of 1-heptacosanol as obtained from the literature

Compound HAJ		**1-Heptacosanol** (Abdi et al., 2020)	
^{1}H-NMR	**^{13}C-NMR**	**^{1}H-NMR**	**^{13}C-NMR**
3.66 (2H, t, J = 6.60, H-1)	62.4 (C-1)	3.66 (2H, t, J = 6.60, H-1)	63.1 (C-1)
1.65 (4H, m, H-2&3)	32.5 (C-2)	1.61 (4H, m, H-2&3)	32.8 (C-2)
	31.9 (C-3)		31.9 (C-3)
1.24(46H, br s, H-4 to H-26)	29.7-29.3(C4-24)	1.27(46H, br s, H-4 to H-26)	29.7-29.3(C4-24)
	25.7 (C-25)		25.7 (C-25)
	22.7 (C-26)		22.6 (C-26)
0.88 (3H, t, J = 6.8, H-27)	14.1 (C-27)	0.89 (3H, t, J = 6.8, H-27)	14.1 (C-27)

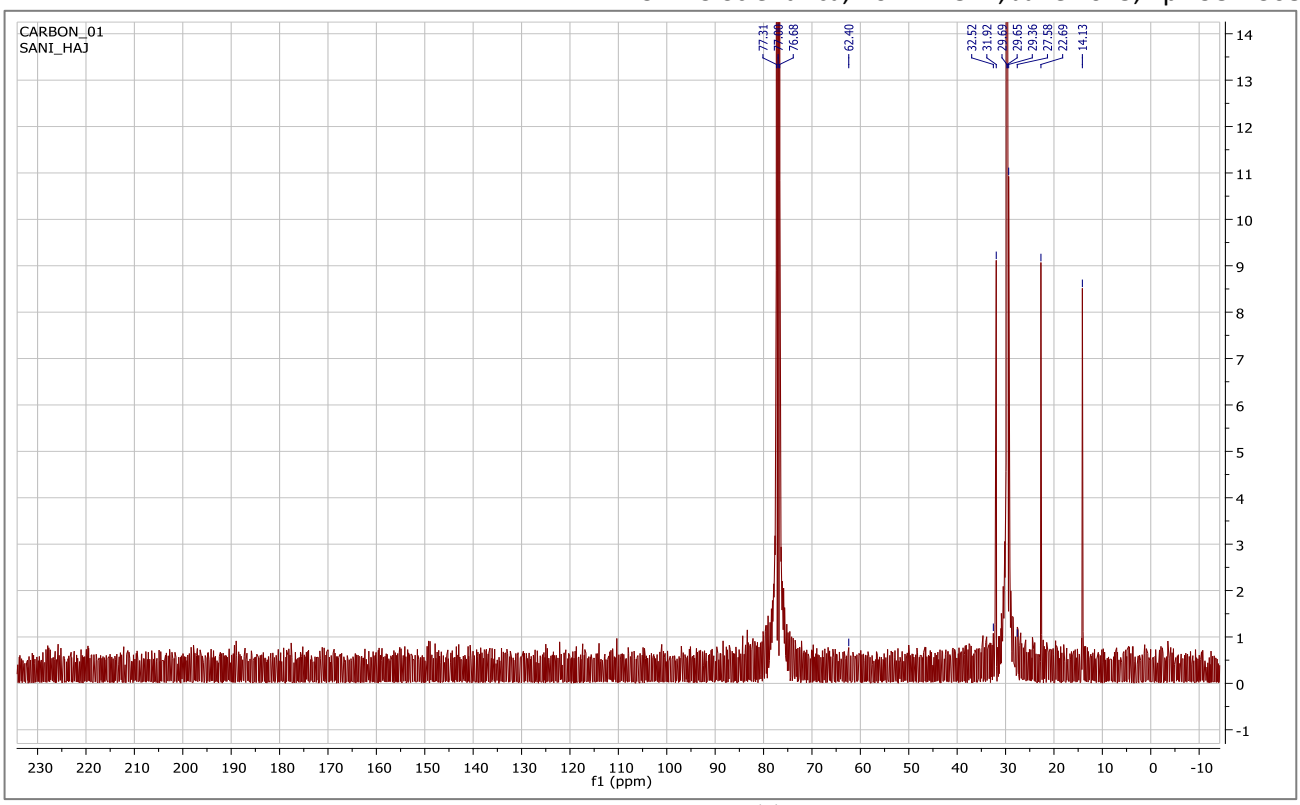

Figure 4: ^{13}C-NMR Spectrum of Compound HAJ Isolated from *T. viride* in Deteurated Chloroform

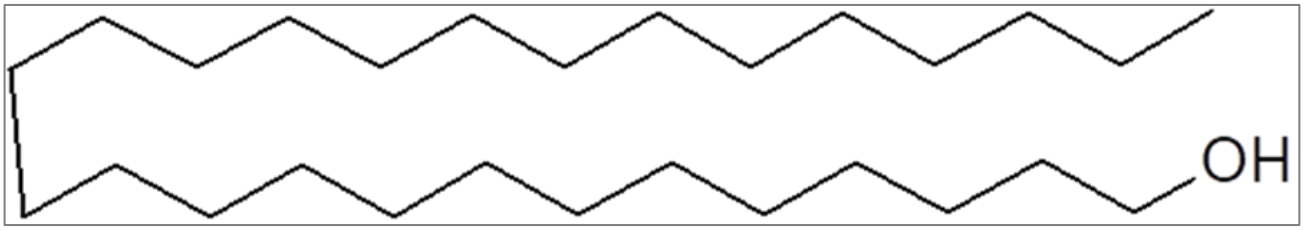

Figure 5: Chemical Structure of Compound HAJ (1-heptacosanol) Isolated from *T. viride*

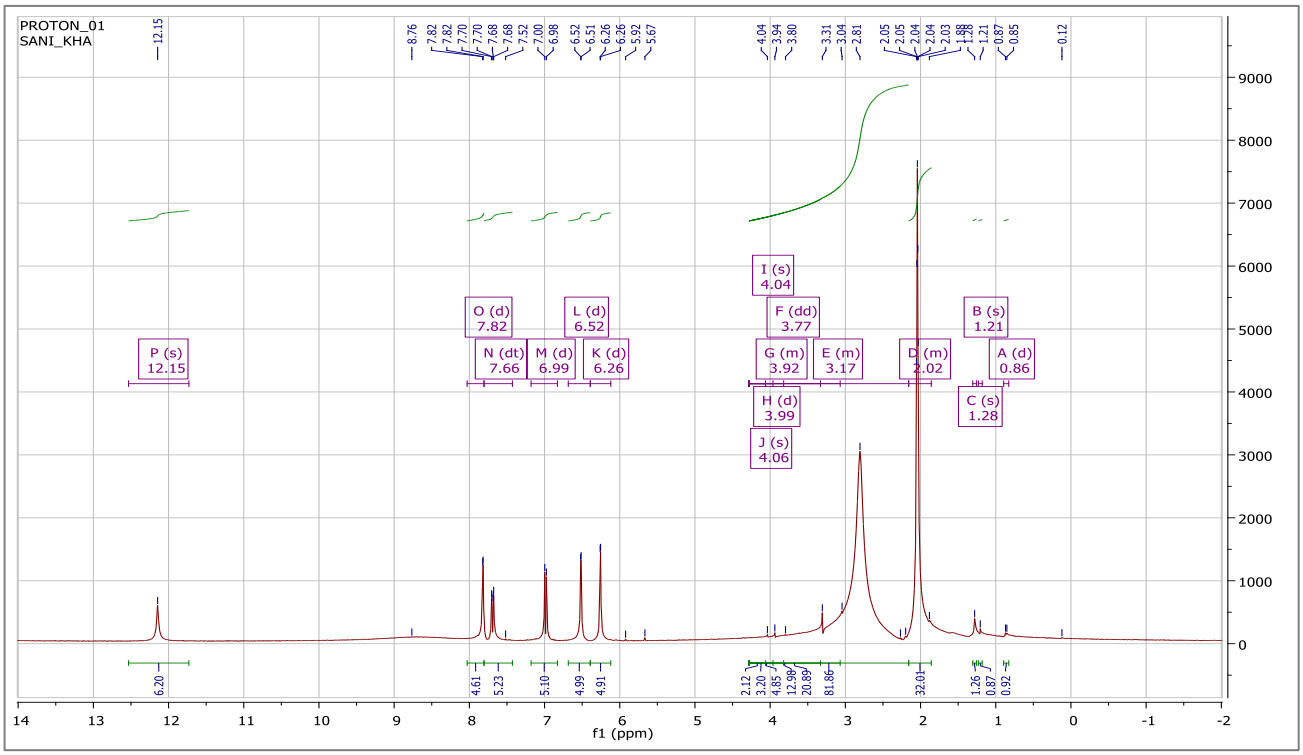

Figure 6: Proton NMR Spectra of KHA Isolated from *T. viride* in Deteurated Acetone

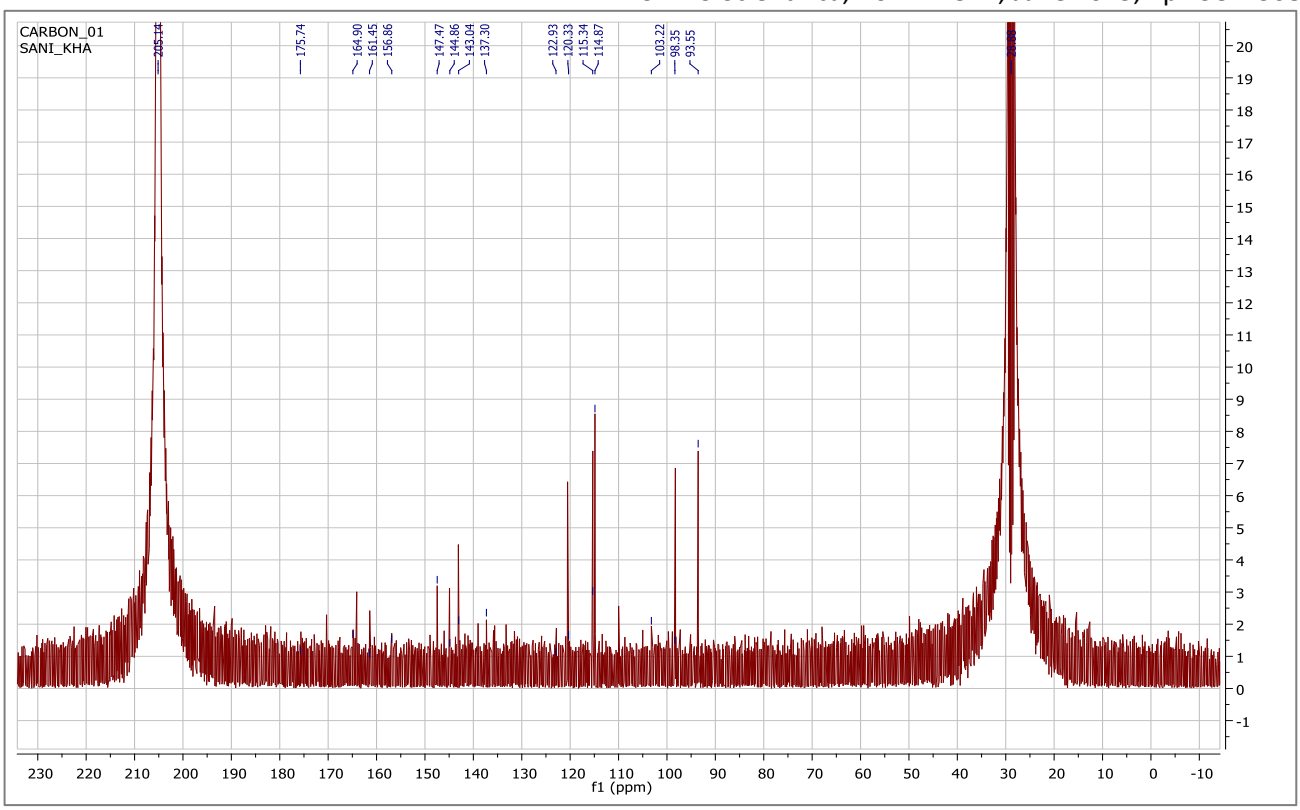

Figure 7: ^{13}C-NMR Spectrum of Compound KHA Isolated from *T. viride* Deteurated Acetone

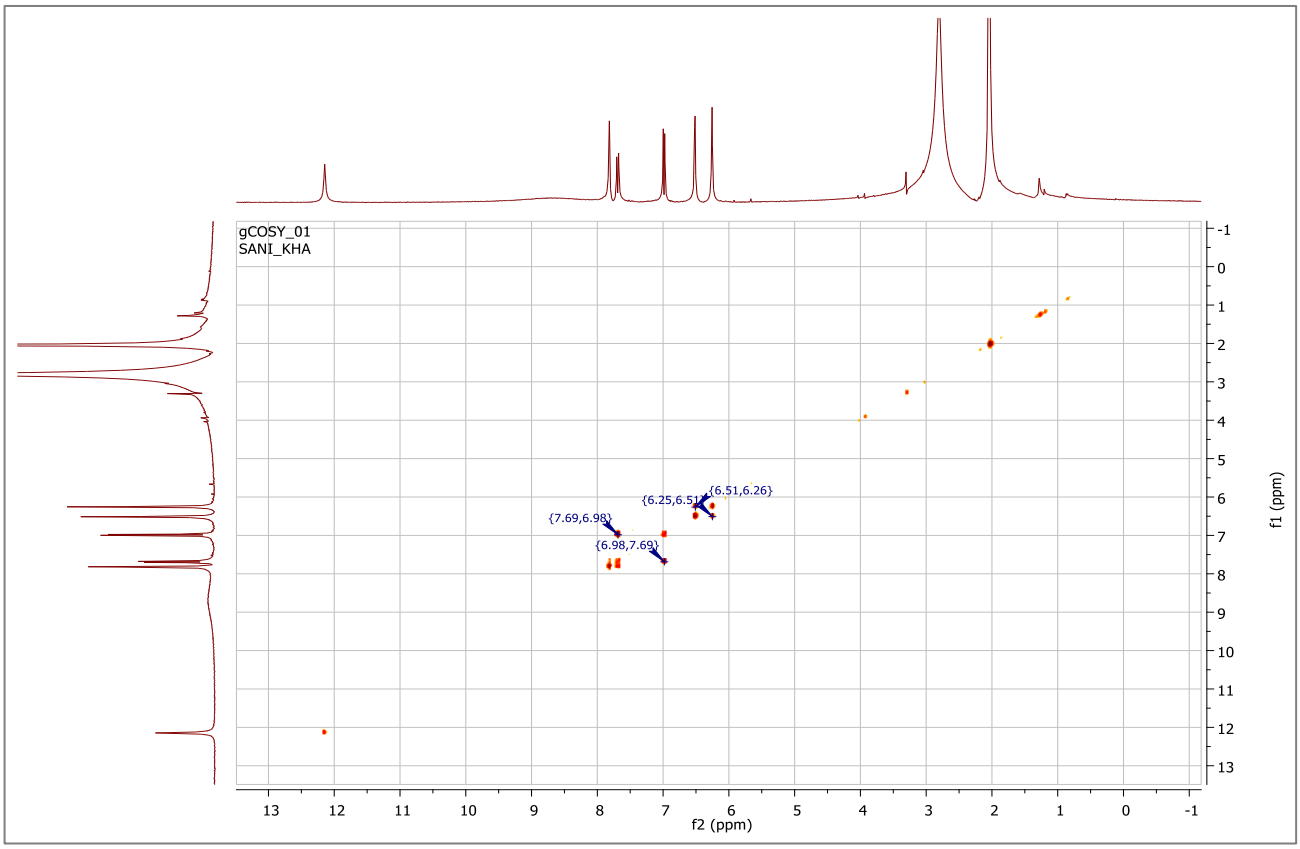

Figure 8: COSY Spectrum of Compound KHA Isolated from *T. viride* Deteurated Acetone

NMR spectra of compound KHA isolated from *T. viride*

^{1}H NMR spectrum of compound KHA

The ^{1}HNMR suggested five aromatic protons δ 6.26 (d, *J* =2.1), 6.52 (d, *J* =2.1), 6.99 (d, *J* =8.7), 7.67 (d, *J* =2.2), and 7.82 (d, *J* =2.2) ppm, all of which are doublets. Hydroxyl protons were also present at δ 4.04, 4.06, 8.79, and 12.15 ppm. The sharp signal at low field at δ 12.15 is consistent with the strong hydrogen bonding between the hydroxyl group and a carbonyl group as shown in Figure 6.

^{13}C NMR spectrum of compound KHA

The ^{13}CNMR showed the carbon signal for carbonyl at δ175.6, which can be assigned to position at C-4. Other carbon signals were as follow; δ147.6 (C-2), δ137.3 (C-3), δ175.6 (C-4), δ161.5 (C-5), δ98.3 (C-6), δ164.0 (C-7), δ93.6 (C-8), δ156.5 (C-9), δ103.2 (C-10), δ122.9 (C-1'), δ114.9 (C-5'), δ143.1 (C-3'), δ145.1 (C-4'), δ115.3 (C-2'), δ120.53 (C-6') as in Figure 7.

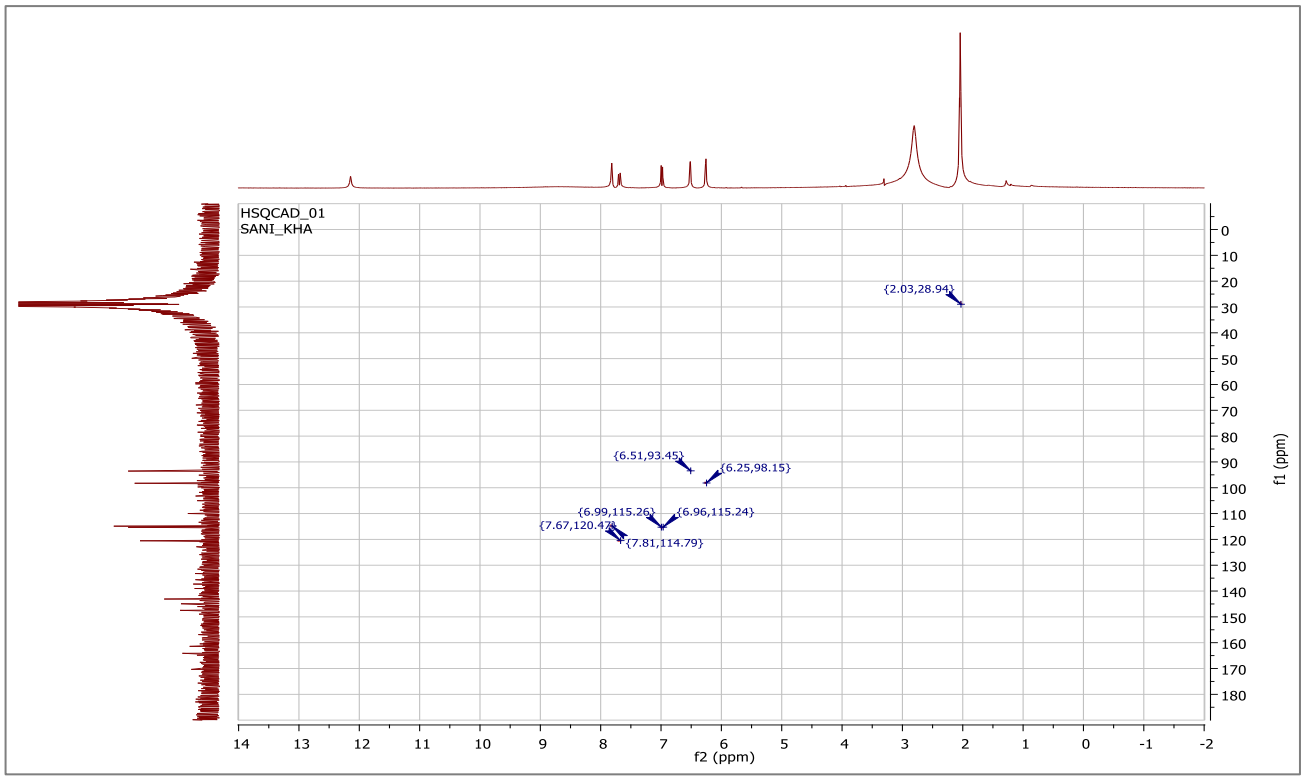

Figure 9: HSQC Spectrum of Compound KHA Isolated from *T. viride* Deteurated Acetone

Table 4: Comparison between Chemical Shift Data of KHA from *T. viride* and that of Quercetin as obtained from Literature

	KHA		Quercetin (Liu *et al*., 2010)	
C	δ-^{13}C	δ-^{1}H	δ-^{13}C	δ-^{1}H
2	147.6		147.9	
3	137.3		135.9	
4	175.6		176.0	
5	161.5		160.9	
6	98.3	6.26 (d, *J* =2.1)	98.4	6.17 (d, *J* =2.0)
7	164.0		164.1	
8	93.6	6.52 (d, *J* =2.1)	93.5	6.39 (d, *J* = 2.0)
9	156.5		156.3	
10	103.2		103.2	
1´	122.9		122.1	
2´	115.3	6.99 (d, *J* =8.7)	115.8	6.87 (d, *J* = 8.5)
3´	143.1		145.2	
4´	145.1		147.0	
5´	114.9	7.82 (d, *J* =2.2)	115.2	7.66 (d, *J* = 2.0)
6´	120.53	7.67 (d, *J* =2.2)	120.2	7.53 (d, *J* =2.0)

COSY spectrum of compound KHA

In the COSY spectrum, coupled peaks were observed between δH 7.67 and δH 6.99, and between δH 6.26 and δH 6.52, as shown in Figure 8.

HSQC spectrum of compound KHA

The HSQC spectrum showed H-C correlations (ie, which proton is attached to which carbon) in compound KHA, such as between δH 6.25 to δC 98.1, δH 6.51 to δC 93.6, while δH 7.81 to δC 114.9, δH 6.99 to δC 115.3, and δH 7.67 to δC 120.5. Details are as shown in the HSQC spectrum in Figure 9.

DISCUSSION

Flavonoid-rich fraction shows absorption maxima at 256, 368, 505, and 658nm whereas the column fraction B&C shows a double peak at 255 and 371 nm. Table 2 displays the highest absorption wavelength and the number of

peaks. By measuring the electronic transition of π-bonds, σ-bonds, and lone pairs of electrons, the UV–VIS spectrophotometry was utilised to identify the existence of aromatic rings and chromophoric groups in fractions. Phenolics and alkaloids are confirmed by the qualitative UV-VIS profile of the *T. viride* flavonoid-rich fraction examined in the 200–800 nm wavelength region (Leelavathi & Udayasri, 2018).

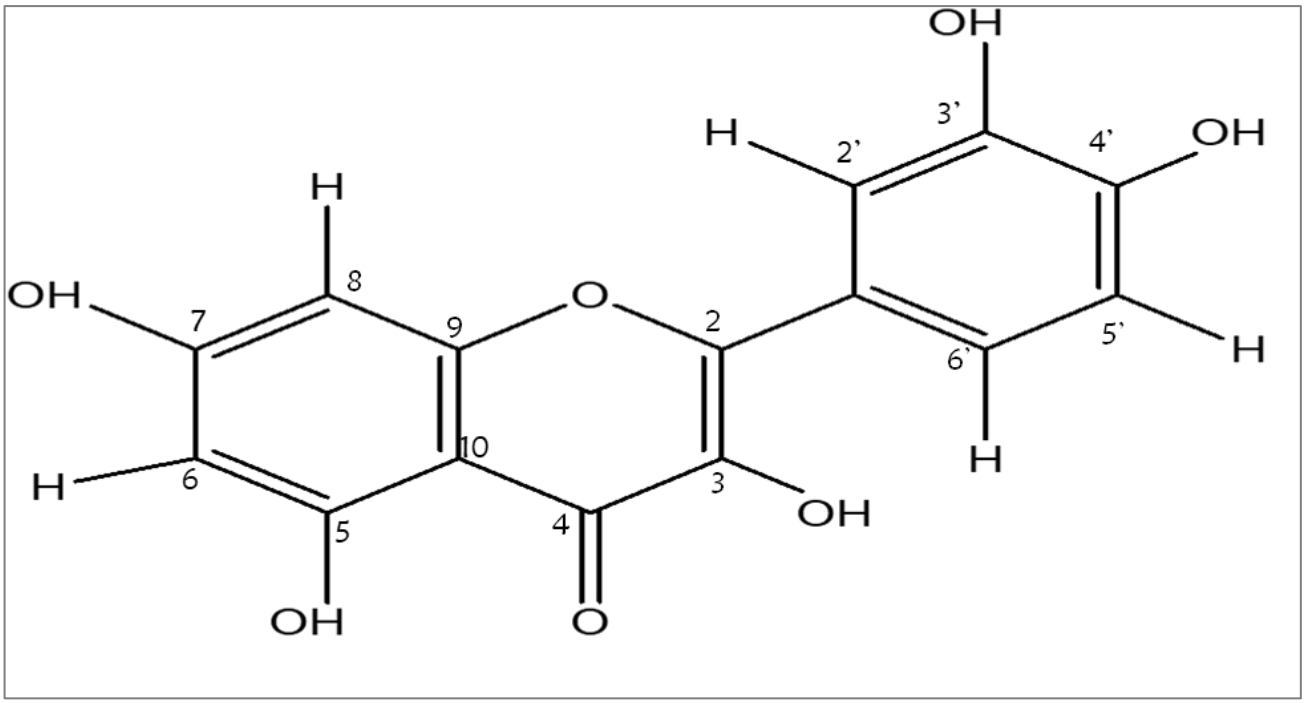

Figure 10: Chemical Structure of Compound KHA (Quercetin) Isolated from *T. viride*

Important peaks in the flavonoid-rich and column fractions are 256/368 nm and 255/371 nm, respectively, which are attributed to flavonoids. Anburaj and Jothiprakasam (2017) reported that two absorption maxima in the 230–290 nm (band II) and 300–350 nm (band I) ranges are commonly found in flavonoid spectra. The absorption maxima of flavones and flavonols are around 310–370 nm, and the wavelength of flavonols is often longer than that of flavones (Cobzac et al., 2019). The B-ring cinnamonoyl system is thought to be responsible for absorption in band II, whereas the A-ring benzoyl system is thought to be responsible for absorption in band I (Kumar & Pandey, 2013; Mabry *et al.*, 1970). Kaempferol 4' -methyl ether, a flavonoid isolated from the plant by Shehu *et al* (2016b) was reported to have a peak of band I at 367nm (Mabry et al., 1970). In column fraction peak absorption at 255 nm and 371 nm, which corresponds to that of Quercetin (Kumar & Pandey, 2013; Tsimogiannis *et al.*, 2007). An additional absorption maximum at 505 and 658 nm in the flavonoid-rich fraction is a spectral fingerprint of chlorophyll and carotenoid compounds (Ashenafi et al., 2023).

The fundamental details about the molecular structure of organic molecules in plant extracts may be obtained using FTIR, a potent, flexible, and non-destructive analytical method used for chemical characterisation of various substances (Patle et al., 2020). To determine the distinctive absorption peaks that correspond to the stretching vibrations of various functional groups, the infrared spectra of flavonoid-rich and column fractions in the frequency range of 4000-650 cm^{-1} are acquired, as illustrated in Figures 1 and 2, respectively. A functional group was indicated by the emergence of FTIR bands in the 4000–1500 cm^{-1} range, and the fingerprint area was identified by the presence of significant absorption bands in the 1500–500 cm^{-1} range. The O-H frequencies are located between 3700 and 3200 cm^{-1}, while the C-H stretching vibrations took place between 2900 and 2800 cm^{-1} (Karpagasundari & Kulothungan, 2014).

One notable distinctive peak in the flavonoid-rich fraction, located between 3694 and 3240 cm^{-1}, was attributed to the O-H group's stretching vibration. The absorption band for the compound's CH_2 asymmetric and symmetric stretching groups was found in the 2922 and 2855 cm^{-1} area. The strong bands at this region indicate the presence of methylene (CH_2) groups in compound(s) within the fraction. The carbonyl C=O stretching vibration is attributed to the prominent band seen at 1654 and 1603 cm^{-1}. The Ar-H group substitutions were suggested by the bending vibration for O-H at 1443 cm−1 and the band at 787 cm^{-1}.

For column fraction, the carbonyl C=O stretching vibration was attributed to the significant band seen at 1655 and 1606 cm^{-1}. A noticeable peak for O-H at 1500–1400 cm^{-1}. The C-O-C group's stretching vibration was suggested by the strong peak at 1163–1092 cm^{-1}, while the Ar–H group substitutions were shown by the band at 800–600 cm^{-1}. Therefore, FTIR is utilised to identify the functional groups found in various phytochemicals. In comparison with that of the flavonoid-rich fraction, the column fraction has no band around the CH_2 asymmetric and symmetric stretching group region (2922 and 2855

cm^{-1} in the flavonoid-rich fraction), which may have been eluted as compound HAJ.

Methylene protons on oxygenated carbon, designated as position-1, were identified by the triplet signal at δ 3.66 (2H, J = 6.8 Hz) in the H-NMR spectrum (in $CDCl_3$). Another signal at δ 1.65 (4H, m) was also seen in the spectrum (Figure 3), and it was attributed to four protons on two methylene carbons next to carbon-bearing oxygen. At δ 1.27 (46H, br), it is clear that there are several methylene protons integrating for 46 hydrogens. This demonstrates unequivocally the existence of overlapping signals because the compound's structure contains several methylenes. A terminal methyl group at position-27 may be detected by the upfield signal at δ 0.88 (3H, t, J = 6.8 Hz).

The carbon signals in the ^{13}C-NMR spectrum (figure 4) are caused by a methyl group and methylenes. The oxygenated methylene carbon is responsible for the downfield signal seen at δ 62.4. The information acquired from the proton NMR spectra is consistent with this. Additionally, signals from methylene carbons in the aliphatic areas at δ 32.8, 31.9, 29.7, 29.6, 29.4, 29.3, 25.7, and 22.7 were seen in the spectrum. The existence of seventeen overlapping methylene carbons, which coincided with the ^{1}H-NMR, is what caused the strong signal seen at δ 29.7. Additionally, the terminal methyl group's distinctive signal is the carbon at δ 14.1.

The long-chain alcohol 1-heptacosanol (molecular formula: $C_{27}H_{56}O$, molar mass: 396.73 g/mol), whose structure is proposed in Figure 5, is the subject of the NMR spectrum data produced for chemical HAJ. Table 3 illustrates the similarity between the NMR spectrum data of chemical HAJ and that published for 1-heptacosanol (Abdi et al., 2020). Based on the literature, this compound has not been reported from any species of *Thesium*. Several studies reported the presence of 1-heptacosanol in the flowers of *Hibiscus sabdariffa* (Inikpi et al., 2014), *Hibiscus syriacus* (Sánchez-Hernández et al., 2021), leaf of *Calotropis procera* (Kutelu & Okwute, 2019), leaf of *Senna italica* (Gololo et al., 2016), bulb of *Allium chinense* (Rhetso et al., 2020), and other plants.

The fatty alcohol molecule 1-heptacosanol is found in plants, marine algae, and cuttlefish, namely Sepiella inermis (Vambe et al., 2020). It belongs to a group of compounds called "policosanol", other compounds belonging to the class are 1-tetracosanol (C-24), 1-hexacosanol (C-26), 1-octacosanol (C-28), 1-nonacosanol (C-29), 1-triacontanol (C-30), 1-dotriacontanol (C-32), and 1-tetratriacontano (C-34) (Jang *et al.*, 2019). The presence of 1-heptacosanol in the plant's extract may indicate that the plant has strong antibacterial, nematocidal, antioxidant, and antidiabetic qualities (Fathi and Ghane, 2022; Vambe *et al.*, 2020). Flavonoid-rich fractions are typically associated with polar compounds due to hydroxyl groups on the flavonoid structure; they may also contain nonpolar compounds. The presence of 1-heptacosanol in the flavonoid-rich fraction may be attributed to the minimal influence of the hydroxyl group on the polarity of the molecule.

The ^{1}H NMR spectrum of compound KHA showed aromatic protons with two *meta*-coupling, one at a doublet at δ 6.26 (H-6) / 6.52 (H-8) and δ 7.82 (H-5′) and 7.67 (H-6′). Strong hydrogen bonding between the hydroxyl group at C-5 and a carbonyl group at C-4 results in a sharp deshielded singlet at δ 12.15. Other hydroxyl protons were observed at 4.04, 4.06, and 8.79 associated with C-3′, C-4′, and C-7, respectively, as shown in Figure 6.

The structure of KHA was further substantiated by ^{13}C NMR experiment, as shown in Figure 7. A highly de-shielded ^{13}C signal at δc 175.6 ppm indicates the carbonyl carbon at C-4, a benzylic carbon (C-2) at δ 147.6, and oxygen-bonded ethylenic carbon (C-3) at δ 137.3. All the protons were carefully assigned to their respective carbon atoms using the HSQC spectra in Figure 9.

Based on available data and in comparison with available data (Liu *et al.*, 2010) on Table 4, KHA was assigned to the structure of 5,7,3',4'-flavon-3-ol commonly known as Quercetin (molecular formulae: $C_{15}H_{10}O_7$, molar mass: 302.23 g/mol) as shown on Figure 10. The slight variation in the chemical shift of the NMR signal, especially the aromatic protons, can be attributed to the solvent used. The literature NMR data of quecetin was dissolved in DMSO, which is known to shift the hydroxyl proton signal downfield due to its hydrogen bonding ability, which can directly affect the neighbouring aromatic proton signal, causing them to shift slightly upfield (to a lower ppm value) due to the deshielding effects from the hydroxyl group.

From the literature review, this compound has not been reported or isolated from the plant *T. viride*. Other species of the genus were reported to contain Quercetin and its glycosides, such as quercetin rhamnosylrhamnosyl-glucoside, quercetin robinobioside, quercetin pentoside hexoside, quercetin-O-dihexoside, and quercetin-O-hexoside (Lombard et al., 2022). Quercetin, a common flavonol found in plants. It has a number of biological properties, including antibacterial, antiparasitic, anti-inflammatory, cardiovascular protective, and anti-immunosuppressive properties (Yang *et al.*, 2020). Scavenging of superoxide anions was the primary mechanism by which various flavonoids, including Quercetin, myricetin, and rutin, exhibited their antioxidative activities (Yen & Chen, 1995). Phase 3 research has examined Quercetin, which is derived from plants, as an antioxidant for liver illness. Antioxidative treatment has a long way to go, even with some encouraging clinical trial findings. Actually, a lot of antioxidants work quite well for treating or preventing diseases in animal models, but they don't seem to work well for treating known illnesses in humans (Jiménez-Arellanes et al., 2016).

CONCLUSION

The study has established the spectroscopic fingerprints of flavonoid-rich fraction for quality control and isolation of 1-heptacosanol and Quercetin from *T. viride* for the first time, which can be subjected to further biological assays.

ACKNOWLEDGEMENT

We gratefully acknowledge the Tertiary Education Trust Fund (TETFUND) for sponsoring this research under the 2024 Institutional Based Research (IBR) initiative through Kaduna State University, Kaduna.

REFERENCES

Abdi, B., Getaneh, E., Assefa, T., Dekebo, A., Tesso, H., Abdo, T., & Melaku, Y. (2020). Chemical Constituents of the Roots Extract of *Dryopteris schimperiana* and Evaluation for Antibacterial and Radical Scavenging Activities. *Ethiopian Journal of Science and Sustainable Development, 7*(1), 1–8. [Crossref]

Anburaj, R., & Jothiprakasam, V. (2017). Bioassays of tannin rich fraction and identification of compounds using UV-Vis, FTIR and RP-HPLC. *Research Journal of Pharmaceutical, Biological and Chemical Science, 8*(1), 432–445.

Ashenafi, E. L., Nyman, M. C., Shelley, J. T., & Mattson, N. S. (2023). Spectral properties and stability of selected carotenoid and chlorophyll compounds in different solvent systems. *Food Chemistry Advances, 2*(2023), 100178. [Crossref]

Cobzac, S. C. A., Casoni, D., Babea, M., Balabanova, B., & Ruzdik, N. M. (2019). Ultraviolet-visible (Uv-vis) spectroscopy and cluster analysis as a rapid tool for classification of medicinal plants. *Studia Universitatis Babes-Bolyai Chemia, 64*(4), 191–203. [Crossref]

Donkor, S., Larbie, C., Komlaga, G., & Emikpe, B. O. (2019). Phytochemical, Antimicrobial, and Antioxidant Profiles of *Duranta erecta* L. Parts. *Biochemistry Research International, 2019*(1). [Crossref]

Fathi, M., & Ghane, M. (2022). Phytochemical Composition, Antibacterial, and Antibiofilm Activity of *Malva sylvestris* Against Human Pathogenic Bacteria. *Jundishapur Journal of Natural Pharmaceutical Products, 17*(1), 1–9. [Crossref]

Gololo, S. S., Mapfumari, N. S., Sethoga, L. S., Olivier, M. T., Shai, L. J., & Mogale, M. A. (2016). Identification of Phytochemical Constituents within the *N*-Hexane Leaf Extract of *Senna italica* (Mill) using Gas Chromatography-Mass Spectrometry (GC-MS) analysis. *Journal of Pharmaceutical Sciences and Research, 8*(10), 1141–1143.

Guemari, F., Laouini, S. E., Rebiai, A., Bouafia, A., & Barhoum, A. (2022). UV-Visible Spectroscopic Technique-Data Mining Tool as a Reliable, Fast, and Cost-Effective Method for the Prediction of Total Polyphenol Contents: Validation in a Bunch of Medicinal Plant Extracts. *Applied Sciences, 12*, 9430. [Crossref]

Inikpi, E., Lawal, O. A., Ogunmoye, A. O., & Ogunwande, A. (2014). Volatile composition of the floral essential oil of *Hibiscus sabdariffa* L. from Nigeria. *American Journal of Essential Oils and Natural Products, 2*(2), 4–7.

Iwu, M. M. (2014). *Handbook of African medicinal plants* (2nd ed.). CRC Press

Jain, P. K., Soni, A., Jain, P., & Bhawsar, J. (2016). Research Article Phytochemical analysis of *Mentha spicata* plant extract using UV-VIS, FTIR and GC/MS technique. *Journal of Chemical and Pharmaceutical Research, 8*(2), 1–6.

Jang, Y., Kim, D., Han, E., & Jung, J. (2019). Physiological Activities of Policosanol Extracted from Sugarcane Wax. *Natural Product Sciences, 25*(4), 293–297. [Crossref]

Jiménez-Arellanes, M. A., Gutiérrez-Rebolledo, G. A., Meckes-Fischer, M., & León-Díaz, R. (2016). Medical plant extracts and natural compounds with a hepatoprotective effect against damage caused by antitubercular drugs: A review. *Asian Pacific Journal of Tropical Medicine, 9*(12), 1141–1149. [Crossref]

Karpagasundari, C., & Kulothungan, S. (2014). Analysis of bioactive compounds in *Physalis minima* leaves using GC MS, HPLC, UV-VIS and FTIR techniques. *Journal of Pharmacognosy and Phytochemistry, 3*(4), 196–201.

Kaur, J., Dhiman, V., Bhadada, S., Katare, O. P., & Ghoshal, G. (2022). LC/MS guided identification of metabolites of different extracts of *Cissus quadrangularis*. *Food Chemistry Advances, 1*, 100084. [Crossref]

Kumar, S., & Pandey, A. K. (2013). Chemistry and Biological Activities of Flavonoids: An Overview. *The Scientific World Journal, 2013*(1). [Crossref]

Kutelu, A. M., & Okwute, S. K. (2019). Phytochemical Analysis, Volatile Components and Biological Evaluation of the leaf of *Calotropis procera* (Asclepiadaceace). *International Journal of Research and Innovation in Applied Science, 6*(12), 60–67.

Leelavathi, V., & Udayasri, P. (2018). Qualitative and Quantitative Analytical Studies for the Screening of Phytochemicals from the Leaf Extracts of *Senna alexandrina* Mill. *International Journal of Pharmaceutical and Clinical Research, 10*(8), 210–215. ijpcr.com

Liu, H., Mou, Y., Zhao, J., Wang, J., Zhou, L., Wang, M., Wang, D., Han, J., Yu, Z., & Yang, F. (2010). Flavonoids from *Halostachys caspica* and Their Antimicrobial and Antioxidant Activities. *Molecules, 15*, 7933–7945. [Crossref]

Lombard, N., Stander, M. A., Redelinghuys, H., Roux, M. M. Le, & Wyk, B. Van. (2022). A Study of Phenolic Compounds and Their Chemophenetic Value in the Genus *Thesium* (Santalaceae). *Diversity, 14*, 590, 1–29. [Crossref]

Mabry, T. J., Markham, K. R., & Thomas, M. B. (1970). The Ultraviolet Spectra of Flavones and Flavonols. *The Systematic Identification of Flavonoids, see 111*, 41–164. [Crossref]

Madeleine, R., Etame, E., Mouokeu, R. S., Stève, F., Poundeu, M., Voukeng, I. K., Laurel, C., Cidjeu, P., Tiabou, A. T., Joel, A., Yaya, G., Anne, R., Ngane, N., Kuiate, J. R., & Etoa, F. X. (2019). Effect of fractioning on antibacterial activity of

n-butanol fraction from *Enantia chlorantha* stem bark methanol extract. *BMC Complementary and Alternative Medicine, 19*(56), 1–7. [Crossref]

Mustapha, F. J., Ella, E. E., Luka, S. A., & Wada, Y. A. (2023). Phytochemical Constituents and GC-MS Profiling of the Whole Plant Ethanol Extract of *Thesium viride* Hill and its Oral Toxicity in Balb/C Mouse Model. *UMYU Journal of Microbiology Research, 8*(1), 31–38. [Crossref]

Patle, T. K., Shrivas, K., Kurrey, R., Upadhyay, S., Jangde, R., & Chauhan, R. (2020). Phytochemical screening and determination of phenolics and flavonoids in *Dillenia pentagyna* using UV–vis and FTIR spectroscopy. *Spectrochimica Acta - Part A: Molecular and Biomolecular Spectroscopy, 242*, 118717. [Crossref]

Rhetso, T., Shubharani, R., Roopa, M. S., & Sivaram, V. (2020). Chemical constituents, antioxidant, and antimicrobial activity of *Allium chinense* G. *Future Journal of Pharmaceutical Sciences, 6*(102). [Crossref]

Sánchez-Hernández, E., Buzón-Durán, L., Lorenzo-Vidal, B., Martín-Gil, J. M., & Martín-Ramos, P. (2021). Physicochemical Characterization and Antimicrobial Activity against *Erwinia amylovora*, *Erwinia vitivora*, and *Diplodia seriata* of a Light Purple *Hibiscus syriacus* L. Cultivar. [Crossref]

Shehu, S., Ibrahim, G., Iliyasu, U., Shehu, S., Nuhu, A., & Abubakar, M. (2017). Evaluation of antiulcer activity of aqueous ethanol extract of *Thesium viride* on ethanol and aspirin induced models in rats. *Bayero Journal of Pure and Applied Sciences, 9*(2), 82. [Crossref]

Shehu, S., & Iliyasu, U. (2017). Pharmacognostic and Physicochemical Analysis of *Thesium viride* Hill. *International Journal of Science for Global Sustainability, 4*(2). [Crossref]

Shehu, S., Abubakar, M., Ibrahim, G., & Iliyasu, U. (2016a). Phytochemical and Antibacterial Studies on Aqueous Ethanol Extract of *Thesium viride* (Santalaceae). *British Journal of Pharmaceutical Research, 11*(2), 1–6. [Crossref]

Shehu, S., Ibrahim, G., Danmalam, U., October, N., Halilu, M., & Abubakar, M. (2016b). Isolation of Kaempferide and Antimicrobial Activity of Fractions of. *African Journal of Pharmaceutical Research & Development, 8*(1).

Shehu, S., Abdurahman, E. M., Danmalam, U. H., Mohammed, A., & Barau, A. I. (2022a). Evaluation of Antioxidant Activity of *Thesium*. *Nigerian Journal of Pharmacy, 56*(2), 276–284. [Crossref]

Shehu, S., Abdurahman, E. M., Danmalam, U. H., Mohammed, A., Shehu, S., & Iliyasu, U. (2022b). Effects of *Thesium viride* Extract and Fractions on Some Liver Biochemical Parameters in CCl_4-Induced Damage in Wistar Rats. *Tropical Journal of Natural Product Research, 6*(6), 1004–1009. [Crossref]

Tsimogiannis, D., Samiotaki, M., Panayotou, G., & Oreopoulou, V. (2007). Characterization of flavonoid subgroups and hydroxy substitution by HPLC-MS/MS. *Molecules, 12*(3), 593–606. [Crossref]

Vambe, M., Aremu, A. O., Chukwujekwu, J. C., Gruz, J., Luterov, A., Finnie, F., & Van Staden, J. (2020). Antibacterial, Mutagenic Properties and Chemical Characterisation of Sugar Bush (*Protea caffra* Meisn.): A South African Native Shrub Species. *Plants, 9*(1331), 1–12. [Crossref]

Yang, H., Zhou, M., Li, H., Wei, T., Tang, C., Zhou, Y., & Long, X. (2020). Effects of Low-level Lipid Peroxidation on the Permeability of Nitroaromatic Molecules across a Membrane: A Computational Study. *ACS Omega, 5*(10), 4798–4806. [Crossref]

Yen, G. C., & Chen, H. Y. (1995). Antioxidant Activity of Various Tea Extracts in Relation to Their Antimutagenicity. *Journal of Agricultural and Food Chemistry, 43*(1), 27–32. [Crossref]

Zhigila, D. A., Verboom, G. A., & Muasya, A. M. (2020). An infrageneric classification of *Thesium* (Santalaceae) based on molecular phylogenetic data. *Taxon, 6*(1), 1–24. [Crossref]

Zuchowski, J., Pecio, Ł., & Stochmal, A. (2014). Novel flavonol glycosides from the aerial parts of lentil (*Lens culinaris*). *Molecules, 19*(11), 18152–18178. [Crossref]